ORIGINAL ARTICLE

Freshwater Biology WILEY

Capturing the spatial variability of algal bloom development in a shallow temperate lake

David A. Ortiz ⬛ | Grace M. Wilkinson

Department of Ecology, Evolution, and Organismal Biology, Iowa State University, Ames, IA, U.S.A.

Correspondence
David A. Ortiz, Department of Ecology, Evolution, and Organismal Biology, Iowa State University, Ames, IA, U.S.A.
Email: dortiz4@wisc.edu

Present address
David A. Ortiz and Grace M. Wilkinson, Center for Limnology, University of Wisconsin – Madison, Madison, WI, U.S.A.

Abstract

1. Algal blooms can have profound effects on the structure and function of aquatic ecosystems and have the potential to interrupt valuable ecosystem services. Despite the potential ecological and economic consequences of algal blooms, the spatial dynamics of bloom development in spatially complex ecosystems such as shallow lakes remain poorly characterised. Our goal was to evaluate the magnitude and drivers of spatial variability of algal biomass, dissolved oxygen, and pH over the course of a season, in a shallow lake in order to better understand the spatial dynamics of algal blooms in these ecosystems.

2. We sampled 98 locations in a small eutrophic lake on a 65-m grid for several parameters (chlorophyll *a*, phycocyanin, dissolved oxygen, pH, and temperature), weekly over 122 days. This was done to estimate the dynamics of variability and spatial autocorrelation during the course of multiple bloom events. We also compared the spatial measurements to a high frequency sensor deployed at a fixed station and estimated the optimal spatial sampling resolution by performing a rarefaction analysis.

3. Spatial heterogeneity of algal pigments was high, particularly during bloom events, and this pattern and the overall severity of the bloom were not well captured with the fixed station monitoring. The pattern of algal pigments and other limnologically important variables (dissolved oxygen and pH) was related to the direction of prevailing winds 24 hr prior to sampling, the shallow northern basin where the main surface inlet is located, and heavy precipitation. Additionally, a dense bed of floating-leaf macrophytes contributed to local patchiness in all variables. Finally, from the rarefaction analysis we found that minimal information about the mean state of the ecosystem was gained after *c.* 30 locations had been sampled.

4. This study revealed how spatially heterogeneous shallow lakes are over the course of a single season, and that the magnitude of variability was highest during biologically intensive periods such as algal blooms. As such, continued research is needed across a range of trophic conditions to better understand the structure of horizontal variability in lakes. Overall, these data demonstrate the need for spatially explicit monitoring to better understand the dynamics and drivers of algal blooms in shallow lakes and to better manage ecosystem services.

1 | INTRODUCTION

Lakes are highly dynamic ecosystems that can undergo rapid physical and chemical changes at an individual location, throughout their water column, and across the entire lake surface at the scale of hours, days, seasons, and years (Laas et al., 2012; Read et al., 2011; Wynne & Stumpf, 2015). Quantifying heterogeneity in aquatic ecosystem structure and function not only improves our understanding of lake ecology and the underlying mechanisms that drive spatial and temporal heterogeneity, but also provides insights that improve management of these ecosystems and the services they provide. With the development of sophisticated sensor technology, high frequency measurements of variables such as dissolved oxygen and temperature have helped limnologists grasp the scale of temporal heterogeneity in lakes (Carpenter et al., 2020; Chaffin et al., 2020; Cotterill et al., 2019). Detailed temporal monitoring has led to advances in understanding several lake mechanisms such as diel cycles in primary production (Solomon et al., 2013; Staehr et al., 2012), temperature effects on biogeochemical processes (Medeiros et al., 2012), and early warnings of the transition to alternative stable states (Carpenter et al., 2011; Wilkinson et al., 2018). Additionally, high frequency measurements have been used to better understand heterogeneity over depth (vertical spatial heterogeneity) for important processes such as stratification (Boehrer & Schultze, 2008; Read et al., 2011). Despite these advances in understanding temporal and vertical heterogeneity, less is known about the dynamics of horizontal spatial heterogeneity in the surface waters of lakes.

The vast majority of our understanding of lentic ecosystem structure and function comes from single station sampling, with measurements taken through time over the deepest point in the lake (Stanley et al., 2019). This location is usually selected to be representative of conditions in the lake; however, the representativeness of a single location is likely to vary with regards to the variable being measured and with time due to interacting forces such as wind, hydrology, bathymetry, and biology (Chaffin et al., 2020; Schilder et al., 2013; Wu et al., 2010; Zhou et al., 2013). For example, ecosystem metabolism measured at dozens of locations for 10 days in two north temperate lakes varied by 1–2 orders of magnitude, with more than three-quarters of the variability attributable to the measurement location within the lake (Van de Bogert et al., 2012). Transect-based studies of reservoirs have revealed gradients in algae pigments, pH, and nutrients with differences varying between 25% and 180% within a waterbody (Moreno-Ostos et al., 2009; Rychtecky & Znachor, 2011; Smith, 2018). Recently, satellite-based studies have demonstrated the ability to detect spatial patterns at a high resolution for optical variables in large lakes (Lekki et al., 2019). Despite these advances, relatively few studies have quantified horizontal spatial variability over time in lakes (Butitta et al., 2017; Loken et al., 2019; Vilas et al., 2017), hampering our understanding of the magnitude of heterogeneity in variables important for managing water quality and ecosystem services.

The development of algal blooms is expected to be a spatially heterogeneous phenomenon (Buelo et al., 2018; Butitta et al., 2017; Serizawa et al., 2008) due to both local heterogeneity in nutrient limitation, zooplankton grazing, and temperature (Davis et al., 2009; Hansen et al., 1997) and population scale heterogeneity due to wind (George & Heaney, 1978). Algal blooms can have a negative effect on ecosystem services, and therefore are often a target for ecosystem monitoring and management. Some bloom-forming taxa, particularly freshwater cyanobacteria, can produce toxins that rise to dangerous concentrations for humans, pets, and livestock (Codd et al., 2005; Corbel et al., 2014). Additionally, the mineralisation of settling phytoplankton contributes to anoxic bottom waters, while intense periods of primary production cause large variation in dissolved oxygen and pH (in poorly buffered ecosystems) over the course of the day, which is stressful for aquatic organisms (Gilbert, 2017; Landsberg, 2002). Furthermore, the perceived recreational value of lakes declines when blooms form (Angradi et al., 2018), which in turn can negatively affect local economies (Dodds et al., 2009). Despite the risk of economic loss, loss in biodiversity, and potential human harm, the spatial dynamics of bloom development in spatially complex ecosystems such as shallow lakes remain poorly characterised.

Shallow lakes have a large interface between the sediment and water relative to deeper lakes, making them more susceptible to rapid changes in water residence time and nutrient inputs (Christensen et al., 2013; Rennella & Quiros, 2006; Romo et al., 2013). Due to the expansive littoral zones, shallow lakes can have large macrophyte beds that modify the light climate and turbulence at the sediment–water interface (Andersen et al., 2017; Moller & Rordam, 1985; Vilas et al., 2017). Many shallow lakes are also polymictic, experiencing multiple periods of stratification followed by mixing during the ice-free season. During periods of water column stability, some cyanobacteria taxa thrive, initiating blooms (Carey et al., 2012). Additionally, episodic nutrient loading from the catchment during storm events (Carpenter et al., 2015; Kelly et al., 2019), spatial gradients in nutrient availability due to stream inlets and morphology (e.g. embayments), and wind-driven circulation (Schoen et al., 2014) can all contribute to spatial heterogeneity of algal blooms over time in shallow lakes.

To better understand the spatial dynamics of algal blooms in shallow lakes, we performed intensive spatial sampling on Swan Lake (Iowa, U.S.A.), a spatially complex, shallow, hypereutrophic waterbody with a history of toxic cyanobacteria algal blooms. In addition to measuring algal pigments throughout the lake over the course of 122 days, we also measured temperature, dissolved oxygen, and pH. The spatial sampling captured two bloom events and coincided with high frequency monitoring of the same variables using autonomous sensors deployed at a fixed station (Ortis et al., 2020). Using these data, we addressed the following questions: (1) how does spatial

variability of algae, dissolved oxygen, and pH change over the course of a season; (2) are high frequency measurements at a fixed station an adequate characterisation of surface water dynamics in a shallow lake; and (3) what is the optimal spatial sampling frequency to capture the mean state of a productive waterbody? Evaluating these questions with data from a spatially complex, hypereutrophic lake will provide valuable ecological and management-relevant insights into algal bloom dynamics.

2 | METHODS

2.1 | Study site

Swan Lake (42.0396, −94.8454) has an average depth of 2 m, surface area of 40.5 ha, and a shoreline development index value of 1.54 (more irregular shape as compared to a perfect circle with the same surface area). The catchment is 350 ha with 92% of the land in agricultural use. The estimated water residence time is approximately 1.5 years. During the ice-free period of 2018, Swan Lake had an average total phosphorus concentration of 280 µg/L and a total nitrogen concentration of 1.61 mg/L, making it hypereutrophic (Carlson, 1977). Total nitrogen was measured as the sum of total Kjeldahl nitrogen (method 351.2 v2, US EPA, 1993c) and nitrate + nitrite measured using the cadmium reduction method (method 4500-NO3-F, US EPA, 1993a). Total phosphorus was measured using the ascorbic acid method (method 365.1 v2, US EPA, 1993b). The average total alkalinity during the same period was 139 mg CaCO$_3$/L determined through end-point titration (APHA, 1998). In addition to seasonal algal blooms, Swan Lake also has non-continuous beds of American lotus (*Nelumbo lutea*) and sago pondweed (*Stuckenia pectinata*) that peak in biomass in the latter half of the summer and then begin senescing. The main surface inlet to the lake enters on the western side and the outlet is at the southern edge of the waterbody (Figure 1). There are no known springs feeding the lake.

2.2 | Field methods

The spatial sampling occurred approximately weekly from day of year (DOY) 142 to DOY 264, encompassing the late spring, summer, and early autumn. A total of 16 spatial sampling events occurred over the course of the 122 days. Measurements of chlorophyll *a*, phycocyanin, temperature, dissolved oxygen saturation, and pH were taken 0.25 m below the surface at 98 sampling stations using a YSI Pro DSS multiparameter sonde (Yellow Springs Instrument, Yellow Springs, OH, U.S.A.) suspended over the side of a 3-m long jon boat equipped with an outboard motor. The sensors, which included the fluorometric total algae (chlorophyll *a* and phycocyanin), optical dissolved oxygen, and Ag/AgCl pH sensors, were calibrated weekly prior to each sampling event according to manufacturer instructions. The sampling stations were laid out in a 65 × 65 m grid across the lake (Figure 1) with each location measured in the same
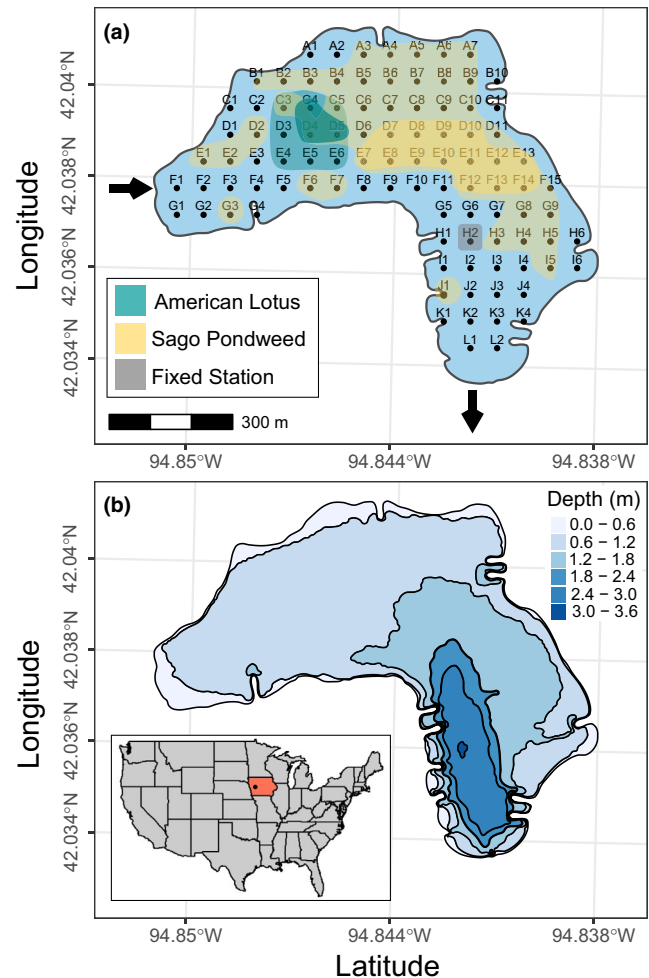
FIGURE 1 Sampling locations on a 65-m square grid of Swan Lake, a 40.5-ha waterbody in western Iowa, U.S.A. The main inlet to the lake and only outlet indicated with arrows. (a) The location of the macrophyte beds of the two dominant species within the lake are shown on the map, with darker shading indicating the regions with the vegetation was always observed, indicating permanent macrophyte beds, and the location of the high frequency sensor, (b) the bathymetry of the lake and location of the lake in the state of Iowa, in reference to the U.S.A.

order (north to south) for each sampling event. This spatial resolution was selected to allow for many sampling locations to be measured in a relatively short window of time, thereby minimising the chance that the differences observed between sampling locations was not due to time of day. Measurements were taken between 10:00 and 14:00, except for the first 2 and last 3 weeks when sampling lasted until 16:00. Beginning on DOY 177 when submerged macrophytes could be identified from the jon boat, the presence or absence of submerged or floating leaf macrophytes was noted at each sampling station during each sampling event. Sampling locations where macrophytes were always noted as present were considered established, permanent macrophyte beds in the lake for that summer. These weekly presence/absence data were used to construct the macrophyte distributions in Figure 1.

The fixed station high frequency monitoring of Swan Lake was performed using a YSI EXO2 (Yellow Springs Instrument) multiparameter sonde equipped with the same sensors as the YSI ProDSS used for the spatial sampling. The sonde recorded measurements of chlorophyll *a*, phycocyanin, dissolved oxygen saturation, and pH every 15 min. The instrument was deployed on DOY 135 over the deepest point in the lake (3.8 m deep), hanging approximately 0.5 m below the surface, and removed on DOY 264 after the spatial sampling event on that day. The fixed station sonde was monitored weekly for drift and calibrated according to manufacturer instructions when indicated by the quality control algorithm in the KorEXO software. Hourly precipitation, wind speed, and wind direction were collected at the Arthur N. Neu Airport in Carroll, Iowa, located 4.5 km from the lake, as a part of the National Oceanic and Atmospheric Automated Surface Observatory System. The meteorological data were used to aid in the interpretation of spatial dynamics over the course of the summer.
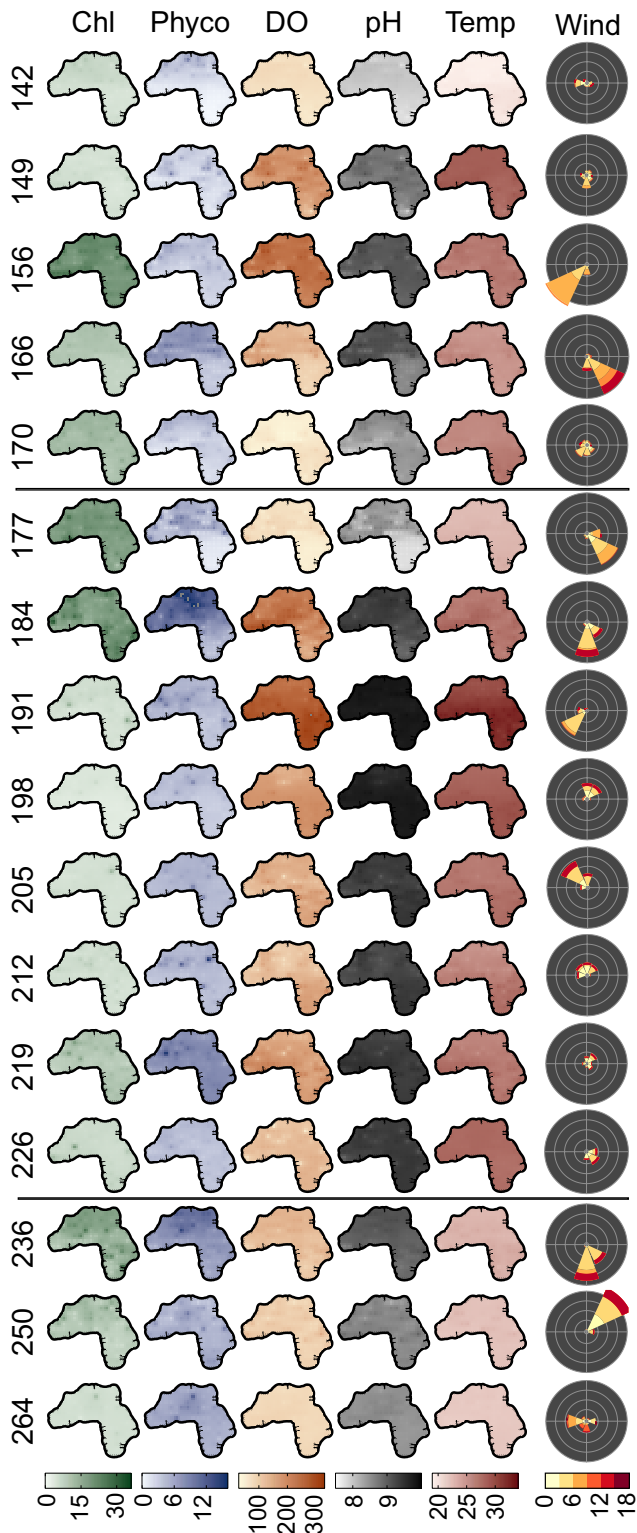
2.3 | Data analysis

Spatial heterogeneity can be quantified by calculating the spatial variance (e.g., coefficient of variation; CV) or spatial autocorrelation (AC; Moran's *I*, Moran, 1950). Increasing spatial variance is indicative of increasing patchiness in the ecosystem, such as areas of high-density algal biomass and areas of low-density biomass within a lake. Spatial AC accounts for the location of those patches within the ecosystem in relationship to each other. Local Moran's *I* quantifies how similar the abundance of algae is at one location compared to the density of surrounding neighbours. When measured over time for variables that are indices of algal biomass (e.g., the pigments chlorophyll *a* and phycocyanin), both of these metrics of spatial heterogeneity can provide insight into the dynamics of algal bloom development. In models of algal blooms, both spatial variance and AC are expected to be high during the bloom period (Buelo et al., 2018).

Spatial AC and the CV were calculated for each variable on each sampling date in order to evaluate the dynamics of these parameters over time. Prior to analysis, extreme outliers in the algal pigments were removed from the spatial dataset as they were well outside the operating range of the Total Algae sensor or there was known interference with the sensor resulting in an inaccurate measurement. This resulted in five chlorophyll *a* and three phycocyanin measurements being removed out of 3,136 total pigment measurements. The spatial CV is the standard deviation (*SD*) of all of the spatial measurements for a variable on a given sampling date divided by the mean of those measurements, expressed as a percent. Spatial AC was calculated as the average value of local Moran's *I* with a queen's distance neighbour list (92 m) with equal weight ($1/n$) on neighbours, as to not impose any assumptions on possible spatial patterns in the variables. We limited our analysis to surrounding neighbours because distances beyond this have not shown high spatial AC of algal pigments under experimental conditions (Butitta et al., 2017). Local Moran's *I* values

near 1.0 reflect high spatial AC within neighbours, zero indicates a random distribution, whereas spatial AC values nearing −1.0 indicate a perfectly dispersed distribution (e.g. checkerboard pattern) in the variable being measured. As the spatial variability in temperature is mediated by physical processes, we used the dynamics and extent of the spatial AC of temperature as a benchmark to visually compare the dynamics of spatial AC in the other biological variables. This allowed us to tease apart the effect of physically versus biologically driven spatial patterns. Additionally, to better visualise the spatial patterns in chlorophyll *a*, phycocyanin, temperature, dissolved oxygen, and pH over the course of the season, the data were interpolated using inverse distance weighting across a 25-m grid (Figure 2).

To evaluate if high frequency measurements at a fixed station are an adequate characterisation of the surface water dynamics in a shallow lake, we compared the measurements taken by the fixed station sonde during the same time period as a spatial sampling event. High frequency data from the fixed station sonde were trimmed to the period that we sampled the lake spatially. A *t*-test with a Bonferroni correction, to account for the multiple comparisons, was performed to compare the distribution from the 98 sampling stations to the fixed station measurements from the same day for each of the four biologically mediated variables, chlorophyll, phycocyanin, dissolved oxygen, and pH. In addition to comparing fixed sonde values to the spatial sampling, we also used the spatial data to identify locations in the lake that were consistently representative of mean conditions, and therefore ideal locations for fixed station monitoring. We identified locations in the lake for each sampling event that had measurements within the range of ±1 *SD* from the mean for each biologically mediated variable (all variables except temperature). We then collated these locations across all sampling dates to identify which of the 98 sampling locations had measurements that most consistently represented the mean conditions of the lake.

Finally, we performed a rarefaction analysis to evaluate the optimal spatial sampling frequency to capture the mean value of the biologically mediated variables. This was done by randomly selecting *n* number of spatial sampling data points ($n = 2$–97) during a sampling event, calculating the mean value from that subset, and then calculating the root mean square error (RMSE), comparing the mean estimate from the subset to the mean of all sampling points during that event. This calculation was repeated 1,000 times for each value of *n*, and each iteration was then averaged. The averaged RMSE values for each subset of *n* were fit using a local polynomial regression with a smoothing factor of 0.1 and each sampling event's RMSE curve was standardised by subtracting the mean of all iterations (*global mean*) from the mean at *n* number of stations, to aid in visual comparison. The spatial data are available through (Ortiz & Wilkinson, 2019) and the fixed station data are available in Ortiz et al. (2019) and further analysed in Ortiz et al. (2020). All analyses were performed using R 4.0.2 (R Core Team, 2020) using the gstat (Pebesma, 2004), rstatix (Kassambara, 2020), and sf packages (Pebesma, 2018).

FIGURE 2 The spatial pattern of each of the variables chlorophyll *a* (Chl, µg/L), phycocyanin (Phyco, µg/L), dissolved oxygen (DO, percent saturation), pH, and temperature (Temp, °C) for each sampling event. The 98 sampling locations taken in a 65-m grid (Figure 1) were interpolated to a 25-m grid using spatial inverse distance interpolation for visualisation here. The colour ramps for each variable are scaled from the lowest to the highest value observed over the course of the season across all sampling locations. The wind roses are the wind speeds (m/s; colour ramp) and direction the wind came from for the 24 hr prior to a sampling event. The concentric circles are the frequency of winds from that direction for the 24-hr period (expressed as a percentage, largest circle is 80% of the time). In the case of a longer *spoke*, the greater amount of time the wind was from that direction. The horizontal lines between DOY 170 and 177, and DOY 226 and 236 mark the two large precipitation events that occurred between those sampling dates

lowest during this first bloom period (Figure 2), and no cyanobacteria were identified in the sample. The second bloom, peaking on DOY 236, was dominated by the cyanobacterium *Microcystis* spp. There were also two large precipitation events during the summer, occurring after sampling on DOY 170 and lasting through DOY 171, and on DOY 232 (Figures 2 and S1). The maximum wind speed recorded during the first precipitation event was 10.8 m/s coming from the southwest and 11.8 m/s during the second precipitation event coming from the southeast. During the first half of the summer (DOY 142–191) the prevailing winds 24 hr prior to the sampling events were from the south, switched to being predominantly from the north from DOY 198–219, and then varied in direction for the rest of the season (Figure 2). The median wind speed for the first period when winds were from the south was 3.6 m/s (Figure 3b). When the winds switched to being predominantly from the north between DOY 198 and 219, the median wind speed was lower at 2.5 m/s (Figure S1).

3.1 | Spatial dynamics

During the two bloom periods, there was not a latitudinal or longitudinal trend in chlorophyll *a* concentrations; instead, there were patches of high chlorophyll *a* concentration on otherwise low-concentration dates (Figure 2). Unlike chlorophyll *a*, phycocyanin had a strong latitudinal trend with higher concentrations in the northern portion (sample sites A1–G4) of the lake during the first bloom. This spatial pattern is readily observed on DOY 184 but is also noticeable for many of the sampling events during the first bloom (Figure 2). During sampling events with a strong latitudinal gradient in phycocyanin (DOY 166–184 and 236) the mean concentration in the northern portion of the lake was nearly double the concentration in the southern portion of the lake (7.29 and 3.76 µg/L, respectively). On these dates, the prevailing winds 24 hr prior to the sampling event were out of the north (Figure S1), yet the lowest concentrations of phycocyanin were found in the southern portion of the lake. Even when the lake was not blooming, there were patches of high

3 | RESULTS

There were two bloom events during the summer of 2018 in Swan Lake. The first bloom occurred from DOY 156–184 and was dominated by the diatom *Aulacoseira* spp. based on a sample taken on DOY 177 examined under a compound microscope at 400× magnification. The phycocyanin concentrations on DOY 177 were the
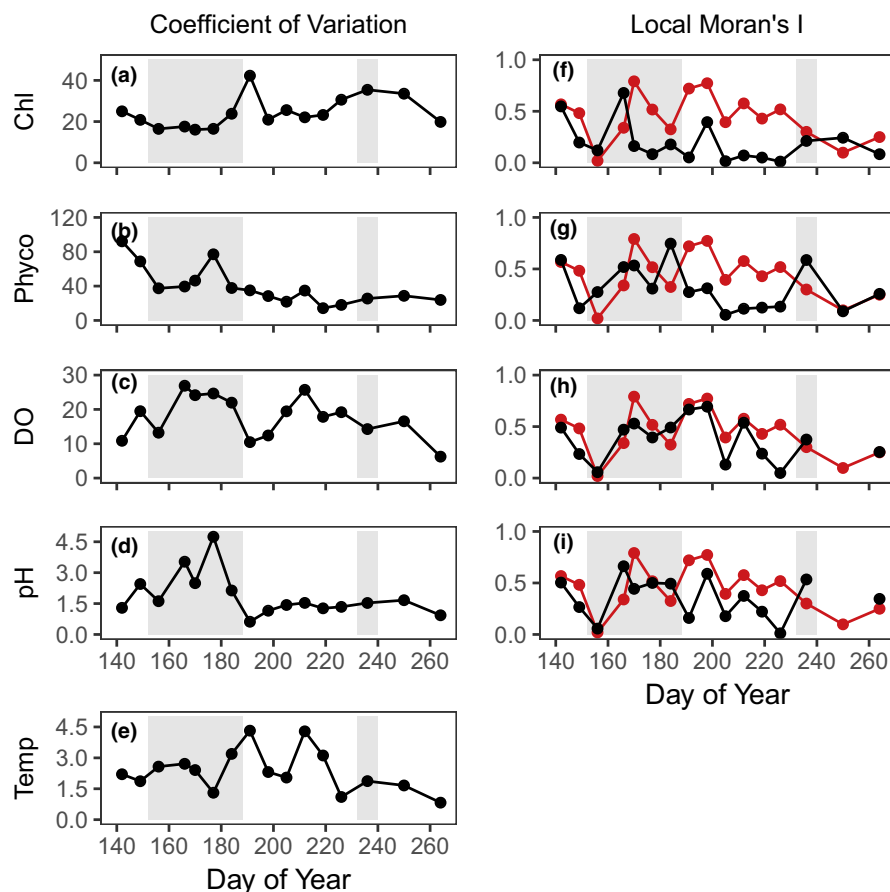
FIGURE 3 Time series of the spatial coefficient of variation (CV) and spatial autocorrelation (AC; local Moran's *I*) of the biologically mediated variables in Swan Lake (same variable abbreviations as Figure 2). The gray polygons indicate periods of algal bloom. The red line is the time series of temperature local Moran's *I* for comparison

concentrations of phycocyanin in the northern portion of the lake (e.g., DOY 212), located among the densest, permanent patch of American Lotus (Figures 1 and S3). The average phycocyanin concentrations at the sampling locations within the American Lotus patch was higher than the average concentration in the rest of the lake for 14 of the 16 sampling events (Figure S2).

The daytime saturation of dissolved oxygen varied the most out of the five variables monitored, ranging from borderline hypoxic (30% saturation) to supersaturated (up to 350%; Figure 2). While the dissolved oxygen saturation increased near the peak of the bloom, the highest average saturation was on DOY 191, after the first bloom had collapsed. There was a weak pattern over the course of the season of higher saturation in the northern portion of the lake, similar to the distribution of higher phycocyanin concentrations. However, within the northern portion of the lake, regions of low dissolved oxygen saturation formed in the surface waters, particularly later in the summer (Figure 1). Beginning on DOY 198, the mean dissolved oxygen concentration in the American lotus patch was consistently lower than the average for the rest of the lake until DOY 250 (Figure S2). The distribution of pH also had a weak spatial pattern during the summer, with slightly elevated values in the northern portion of the lake during the first bloom (e.g. DOY 177; Figure 2). While pH was elevated at the onset of the first bloom period from DOY 149–170, it was highest overall on DOY 191 and 198 after the first bloom had collapsed. Unlike the other variables, temperature had a subtle south to north latitudinal gradient with warmer temperatures

in the southern portion of the lake and colder in the north during the latter half of the summer (Figure 2). On average, this difference between the northern portion of the lake and the southern was 0.5°C. The warmest day of sampling was DOY 191.

Spatial variability in algal pigments during the first bloom event was low, with two exceptions. There was an increase in the CV of chlorophyll *a* on the last day of the bloom (DOY 184; Figure 3a) that continued to increase as the bloom collapsed. There was also a temporary increase in phycocyanin CV during the first bloom on DOY 177 (Figure 3b), coinciding with a temporary decline in phycocyanin concentration across the lake. The CV of both algal pigments was higher than the CV of temperature over the course of the entire sampling period.

Conversely, the CV of pH and dissolved oxygen were elevated during the first bloom period, with pH CV declining and remaining low after the first bloom (Figure 3c) and dissolved oxygen CV only temporarily declining after the first bloom (Figure 3d). Temperature had low variability throughout the first bloom until DOY 177, when the lake began to heat up, peaking in both temperature and spatial variability on DOY 191 (Figure 3e). Between the first and second blooms, DOY 191–226, there was a decrease in spatial variability among the algal pigments and pH as the bloom collapsed, while temperature and dissolved oxygen CV remained relatively high and variable. During the second bloom period, CV was low for all variables except for chlorophyll *a*. In general, the CV of temperature and pH, expressed as a percentage, was an order of magnitude lower than the other variables.

Spatial AC, quantified as local Moran's *I*, did not fall substantially below 0 for any of the variables and peaked at 0.79 among all variables (Figure 3). The highest AC value for chlorophyll *a* and phycocyanin was during the first bloom event (Figure 3f,g); however, phycocyanin AC also increased substantially during the second bloom. During the first bloom, the AC of temperature varied similarly to both pigments' AC, particularly phycocyanin, but became decoupled after the bloom collapsed. While the AC of temperature remained high during the inter-bloom period, the AC of the pigments was substantially lower. Conversely, the dynamics of AC of temperature, dissolved oxygen and pH remained coupled throughout the summer (Figure 3h,i). Dissolved oxygen saturation and pH both increased in AC during the first bloom and then declined throughout the rest of the season with the exception of a minor increase in AC during the second bloom event.

3.2 | Fixed station versus spatial sampling

There were a greater number of days with a significant difference between the spatial and fixed station measurements than days in which the data sets were not significantly different (Figure 4). Among all 64 comparisons (four variables × 16 sampling events), the spatial and fixed station data sets had means that were not significantly different 37.5% of the time. However, the direction of change from week to week was generally consistent between the spatial and fixed station data sets. Phycocyanin had the greatest number of events with similar values, with seven of the 16 sampling events having non-statistically different mean values measured spatially and at the fixed station (Figure 4b). These occurrences were mainly during non-bloom periods. However, even when the

mean phycocyanin values were similar between the sampling methods on a given day, the range of values captured by the fixed station was five times less than the variability captured in the spatial data. This pattern of infrequent occurrences of similar mean values between the two methods during non-bloom periods and a diminished range in the fixed station data, was shared to a degree, among the other three variables as well. Interestingly, dissolved oxygen saturation only had five out of the 16 events with means that were not significantly different, all of which occurred when the lake was above 100% saturation (Figure 4c).

While a majority of the comparisons between the fixed station and spatial data indicate that the algal pigments had a larger range of values in the spatial data, there were a handful of instances where the opposite was true. During the first bloom, the fixed station sonde measured a wide range of chlorophyll *a* concentrations and had a higher mean chlorophyll *a* for all dates (Figure 4a). Similarly, we observed higher mean phycocyanin at the fixed station sonde on DOY 156, 166, 177, 191, and 219 (Figure 4b). However, this pattern did not hold true for dissolved oxygen or pH (Figure 5c,d).

The spatial sampling sites that most consistently captured the mean values in the lake on a given sampling date were in the northwest portion of the lake, near the inlet. The best performing site for all variables was site E3, just west of the American lotus patch and adjacent to a bed of sago pondweed (Figure 1). The four biologically mediated variables from sample site E3 were within the mean (± *SD*) range of all of the spatial measurements 95% of the time. The second-best performing location was in the middle of the American lotus patch, site D4, with the values from this site being within the mean (± *SD*) range 92% of the time. The site where the fixed station was located, site H2, was only within the mean (± *SD*) range 58% of the time.

FIGURE 4 Comparison of the mean (lines and points) and range (shaded polygon) of measurements from the spatial sampling and fixed station measurements. The fixed station data were trimmed to the period that spatial sampling occurred. A filled circle is used for the sampling dates when the means from the two sampling approaches were significantly different ($p < 0.05$), and an open triangle is used for the sampling dates when the mean of the two approaches were not significantly different. The dark blue vertical lines indicate the dates of the two major precipitation events and the red dashed line in panel (c) is at 100% dissolved oxygen saturation
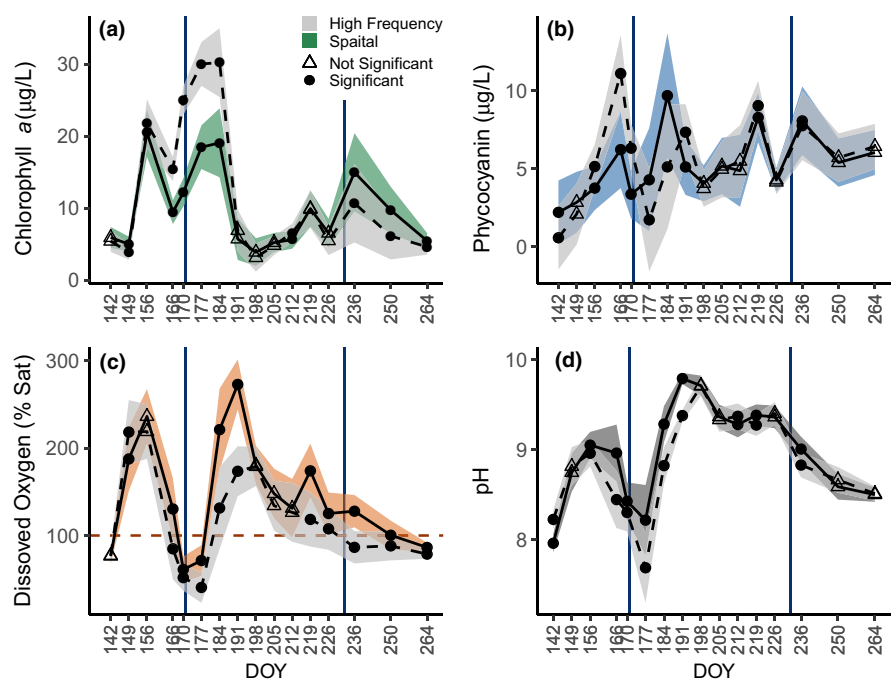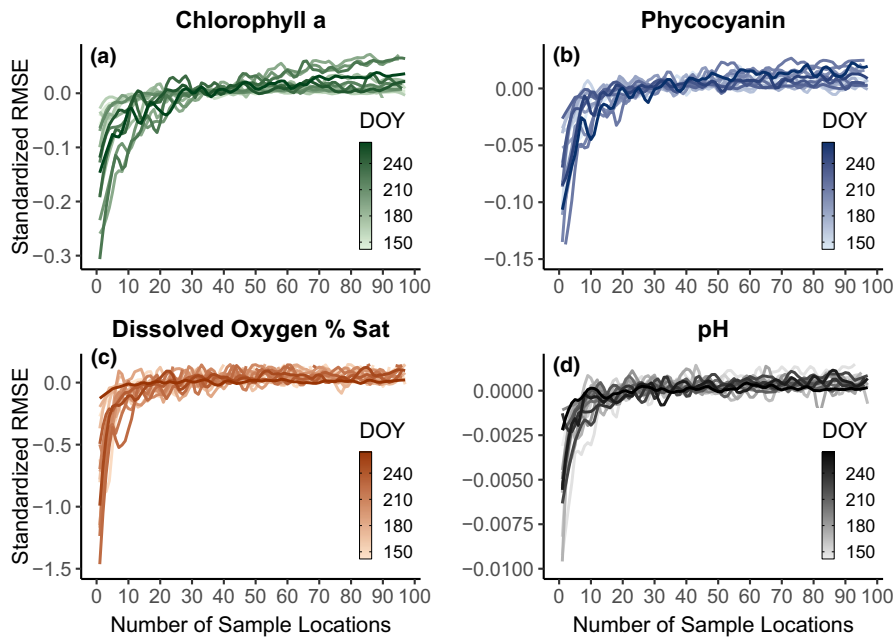
FIGURE 5 Standardised root mean squared errors (RMSE) of rarefaction analysis. Fit lines represent each sampling dates standardised RMSE (16 in total) and the gradient from light to dark indicates first sampling event to last

3.3 | Optimal spatial resolution

To evaluate the spatial sampling resolution needed to capture the mean state of the surface water on a given day, we performed a rarefaction analysis for each variable and each sampling event, calculating the RMSE of a subset of sampling locations compared to the mean value of all 98 measurements that day. The plateaus of the RMSE curves from the rarefaction analysis were used to evaluate the smallest number of spatial sampling locations needed to capture the mean across the lake during that sampling event (Figure 5). Additionally, we also evaluated the temporal pattern of the minimum number of sampling locations needed to capture the mean.

Mean values were underestimated for all variables on all sampling dates when there were less than 10 sampling stations (Figure 5). However, the severity of the underestimation differed among the variables. The rarefaction analysis for chlorophyll *a* indicated that 10–30 sampling locations was sufficient for capturing the mean chlorophyll *a* in Swan Lake, otherwise the mean concentration would be under estimated (Figure 5a). When an algal bloom was occurring, it took more sampling locations to near the mean chlorophyll *a* concentration on that date. However, when the bloom was particularly patchy during development (DOY 226) or collapse (DOY 191), including a larger number of sampling locations led to overestimating the mean chlorophyll *a* concentration as locations with high concentrations were over-represented in the data set. There were similar patterns in phycocyanin RMSE with most sampling dates plateauing between 20 and 30 sampling locations with a few exceptions (Figure 5b). For DOYs 156–170 (rise of the first bloom) and 212, at least 60 sampling locations were needed to capture the overall mean in phycocyanin for that sampling date. Dissolved oxygen saturation and pH were generally well characterised by approximately 10–15 sampling locations as both had a majority of dates in which the RMSE curves plateaued at that spatial

sampling resolution (Figure 5c,d). However, at the beginning (DOY 154), peak (DOY 184), and end (DOY 205) of the first bloom, twice as many sampling locations were needed to capture the mean dissolved oxygen. Only two dates required more sampling locations for pH to capture the mean, DOY 177 and 198, which plateaued at approximately 40 sampling locations. The largest RMSE were observed during bloom conditions for all variables: DOY 177 had the largest error for phycocyanin and pH, while the largest RMSE was on DOY 184 for dissolved oxygen and on DOY 236 for chlorophyll *a* (Figure 5).

4 | DISCUSSION

The spatial heterogeneity of water quality parameters was highly dynamic in Swan Lake, a shallow, hypereutrophic, temperate waterbody. The temporal dynamics in heterogeneity were driven in part by the two blooms, the peaks of which were preceded by large precipitation events. These rain events could have delivered nutrients from the agriculturally dominated catchment into the lake from the northern inlet, helping to fuel the subsequent algal blooms and the spatial patterns observed during blooms (Stockwell et al., 2020). However, there are also a number of other factors that probably contributed to the spatial variability and pattern during and following these bloom events, including the prevailing wind direction prior to sampling, the bathymetry of the basin and location of the surface inlet, and the potential for macrophyte beds to contribute to local patchiness.

The spatial patterns that the algal blooms created were consistent with the expectations from previous modelling and experimental work that spatial AC increases as algal blooms develop (Buelo et al., 2018; Butitta et al., 2017; Serizawa et al., 2008). This pattern was the strongest for phycocyanin, evident by the strong latitudinal

gradient in concentrations during the bloom periods. The sampling dates with phycocyanin concentration gradients (e.g., DOY 166, 177, 184, 236) coincided with persistent winds from the south 24 hr prior to the sampling event, which probably resulted in the higher concentration of algal cells in the northern portion of the lake. The effect of persistent wind directions influencing the distribution of cyanobacteria has also been documented in other shallow eutrophic lakes (Wu et al., 2010). The shallow sediments of the northern basin were also likely to be a source of akinete recruitment (Karlsson-Elfgren & Brunberg, 2004), further contributing to the higher concentrations of phycocyanin in the northern portion of the lake during the first bloom. Augmented nutrient availability in the northern part of the lake due to external loading from the catchment through the surface inlet and internal loading from the sediments overlain by an unstratified water column (Song & Burgin, 2017) may have further amplified the phytoplankton gradient, particularly following precipitation events. Finally, the tendency of the dominant cyanobacteria taxa *Microcystis* spp. to form surface scums probably enhanced the spatial patterns observed with our surface sampling approach.

The sampling dates with a strong gradient of phytoplankton concentrations from north to south also resulted in north–south gradients in water chemistry. On these dates, both dissolved oxygen and pH formed a gradient of high values in the northern portion of the lake and lower values in the south, which would be expected with greater primary production where phytoplankton concentrations were highest. The spatial patterns in the surface water chemistry demonstrate how phytoplankton spatial distribution, driven by wind, can create hot spots and moments of biogeochemical activity within lakes (McClain et al., 2003) that may be missed with traditional, single-station sampling. The dense, permanent patch of floating leaf American lotus macrophytes also created a hot spot of biogeochemical activity.

Macrophyte beds can have a large local influence on water chemistry by inducing stratification, decreasing flow and trapping particles, and modifying the light environment (Green, 2006; Vilas et al., 2017). For 14 of the 16 weeks (87.5%) of the season the phycocyanin concentrations were higher in the bed of American lotus than concentrations elsewhere in the lake. In fact, even on sampling dates when phycocyanin concentrations were otherwise low (e.g., DOY 212), the American lotus patch can be identified based on the phycocyanin concentrations that are nearly twice as high as the rest of the lake. We hypothesise that the macrophyte patch allowed for microstratification in the water column and reduced wind-driven flow. These physical conditions are likely to favour cyanobacteria dominance and the formation of surface scums. Similarly, the dissolved oxygen concentrations in the American lotus patch became consistently lower than the rest of the lake later in the summer, probably due to the plants beginning to senesce, creating a hot spot of decomposition, decreasing both dissolved oxygen and pH (Vilas et al., 2017). While there is not strong evidence in the data that the other submerged macrophyte beds had a similarly strong effect on water chemistry, the data from the American lotus patch illustrate how macrophytes can contribute to local patchiness and overall spatial heterogeneity.

4.1 | Considerations for monitoring

The variables we measured in this study are often the target of water quality monitoring as the dynamics of these variables coincide with changes in ecosystem function and services. Monitoring is often performed at a fixed station over time to capture the dynamics of the ecosystem, but this strategy could potentially result in missed information about the ecosystem's behavior. While the temporal dynamics of all the variables were synchronous between the fixed station and spatial sampling data sets in Swan Lake, our conclusions regarding the magnitude of the blooms and variability in the lake's structure would have been substantially different relying solely on the fixed station data. Among the four biologically mediated variables, only 37.5% of the fixed station estimates of the mean state of the lake statistically matched the estimate from the spatial sampling. The vast majority of those instances (96%) occurred during non-bloom periods, which also coincided with lower wind speed conditions, no prevailing wind direction, and no major precipitation events. The large difference between the spatial sampling and fixed station measurements of algal pigments during blooms was probably driven, in part, by the depth of the sensors at the fixed station and the variable accumulation of cyanobacteria at the surface of the lake dependent upon environmental conditions and the dominant taxa (Chaffin et al., 2020). It is clear from our data that during periods of heightened biological activity such as blooms, fixed station monitoring is unlikely to be representative of the mean ecosystem state in shallow lakes.

Despite the high degree of horizontal spatial variability that has been documented in this study and others (Butitta et al., 2017; Loken et al., 2019; Van de Bogert et al., 2012), fixed station designs are widely used in water quality monitoring programmes. In Swan Lake, we determined that the historical location for water quality monitoring, where the fixed station sensors were deployed, was one of the least-representative locations for mean conditions in the lake. Given the hypereutrophic state of the lake, the most immediate management concerns are toxic cyanobacteria blooms and summer fish kills due to low dissolved oxygen. However, the mean value of these variables (phycocyanin and dissolved oxygen) across the lake were only captured by the fixed station sensors 58% of the time. While selecting a fixed station site for high frequency sensor deployment includes many considerations including the location of previous data collection and management needs, based on our analysis we would advise performing a spatial survey to identify if and when the fixed station site is representative of mean conditions in the lake. A complementary spatial survey will help contextualise the fixed station dynamics and provide additional, management-relevant information about the lake.

It is also important to consider the trade-offs between high frequency fixed station monitoring and higher resolution, but less frequent spatial monitoring. High-frequency monitoring at a single station provides insight into ecosystem function such as metabolism (Staehr et al., 2012), early warnings of impending regime shifts (Carpenter et al., 2011; Wilkinson et al., 2018), and crucial information

on diel variability in limnological conditions (Andersen et al., 2017). However, as we observed in Swan Lake, the spatial variability within a given day often exceeds the temporal variability at a single point in a shallow lake. Without the spatial sampling snapshots, we would have underestimated the magnitude of the algal blooms, hampering our limnological understanding of the ecosystem's functioning and impeding our ability to accurately estimate rates such as methane emissions on a global scale (DelSontro et al., 2018).

From a practical stand point, the understanding gleaned from the spatial sampling could help managers design targeted algal toxin monitoring or management interventions to help control fish habitat quality in persistently hypoxic areas (Bardshaw et al., 2015). However, the time and cost investment in repeated spatial sampling at the resolution performed in this study may not be feasible for both research and management programmes. The rarefaction analysis we performed for all four of the key water quality monitoring variables revealed that minimal information was gained after *c.* 30 locations were sampled across many conditions and variables. Often 12–20 sample locations across the 40.5-ha lake (or a 1–2 samples/ha) was sufficient to capture the spatial variability within the lake, with a few exceptions. These exceptions occurred during times of higher variability such as when the blooms were just starting or when the bloom began to collapse. The need for a higher spatial resolution during bloom events to fully capture their variability has also been found using remote sensing techniques in other, larger lakes (Lekki et al., 2019). As the spatial resolution of remote sensing technologies continues to improve, it may become more cost effective to capture the spatial heterogeneity of algal pigments in small lakes over time. However, one of the benefits of manual spatial sampling is being able to pair other measurements such as dissolved oxygen, pH, and nutrients (e.g., nitrate; Loken et al., 2018; Pellerin et al., 2016) with information on the distribution of algal biomass.

Our intensive spatial monitoring of a shallow, hypereutrophic lake revealed how spatially heterogeneous shallow lakes are over the course of a single season and allowed us to tease apart the drivers of that spatial heterogeneity. We found that variability was greatest during biologically intensive periods, such as during algal blooms and in dense floating-leaf macrophyte beds, and that failure to capture this variability would have hampered our understanding of the ecosystem's functioning and overall mean state. Small lakes such as Swan Lake dominate the global distribution of waterbodies (Verpoorter et al., 2014). Adequately capturing and characterising the magnitude of variability in production of these waterbodies is important given their role in mediating global nutrient cycles (Biddanda, 2017; Downing, 2010), especially methane emissions (DelSontro et al., 2018; Loken et al., 2019). Our data provided an estimate of the spatial resolution needed to capture the dynamics in ecosystems similar to Swan Lake and a method that could be readily adapted to other ecosystems. While our results provide new understanding of the magnitude and temporal dynamics of spatial heterogeneity in shallow lakes, continued investigation of horizontal spatial heterogeneity in a range of aquatic ecosystems, from oligotrophic to eutrophic, is needed to better understand the structure and drivers of horizontal spatial variability in lakes.

CONFLICT OF INTEREST

There are no conflicts of interest to declare.

DATA AVAILABILITY STATEMENT

The data that support the findings of this study are available from Environmental Data Initiative repository: https://portal.edireposit ory.org/nis/mapbrowse?packageid=edi.420.1

ORCID

David A. Ortiz 🆔 https://orcid.org/0000-0003-4605-3530

REFERENCES

American Public Health Association (APHA), American Water Works Association (AWWA), and the Water Environmental Federation (WEF). (1998). *Standard methods for examinations of water and wastewater*, 20th ed. United Book Press, Inc.

Andersen, M. R., Kragh, T., & Sand-Jensen, K. (2017). Extreme diel dissolved oxygen and carbon cycles in shallow vegetated lakes. *Proceedings of the Royal Society B-Biological Sciences*, *284*(1862), 20171427. https://doi.org/10.1098/rspb.2017.1427

Angradi, T. R., Ringold, P. L., & Hall, K. (2018). Water clarity measures as indicators of recreational benefits provided by US lakes: Swimming and aesthetics. *Ecological Indicators*, *93*, 1005–1019. https://doi.org/10.1016/j.ecolind.2018.06.001

Bardshaw, E. L., Allen, M. S., & Netherland, M. (2015). Spatial and temporal occurrence of hypoxia influences fish habitat quality in dense *Hydrilla verticillata*. *Journal of Freshwater Ecology*, *30*(4), 491–502.

Biddanda, B. A. (2017). Global significance of the changing freshwater carbon cycle. *EOS*, *98*, 15–17. https://doi.org/10.1029/2017EO069751

Boehrer, B., & Schultze, M. (2008). Stratification of lakes. *Reviews of Geophysics*, *46*(2), RG2005.. https://doi.org/10.1029/2006rg000210

Buelo, C. D., Carpenter, S. R., & Pace, M. L. (2018). A modeling analysis of spatial statistical indicators of thresholds for algal blooms. *Limnology and Oceanography Letters*, *3*(5), 384–392. https://doi.org/10.1002/lol2.10091

Butitta, V. L., Carpenter, S. R., Loken, L. C., Pace, M. L., & Stanley, E. H. (2017). Spatial early warning signals in a lake manipulation. *Ecosphere*, *8*(10), e01941. https://doi.org/10.1002/ecs2.1941

Carey, C. C., Ibelings, B. W., Hoffmann, E. P., Hamilton, D. P., & Brookes, J. D. (2012). Eco-physiological adaptations that favour freshwater cyanobacteria in a changing climate. *Water Research*, *46*(5), 1394–1407. http://dx.doi.org/10.1016/j.watres.2011.12.016

Carlson, R. E. (1977). Trophic state index for lakes. *Limnology and Oceanography*, *22*(2), 361–369. https://doi.org/10.4319/lo.1977.22.2.0361

Carpenter, S. R., Arani, B. M. S., Hanson, P. C., Scheffer, M., Stanley, E. H., & Van Nes, E. (2020). Stochastic dynamics of Cyanobacteria in long-term high-frequency observations of a eutrophic lake. *Limnology and Oceanography Letters*, *5*(5), 331–336. https://doi.org/10.1002/lol2.10152

Carpenter, S., Booth, E., Kucharik, C., & Lathrop, R. (2015). Extreme daily loads: Role in annual phosphorus input to a north temperate lake. *Aquatic Sciences*, *77*(1), 71–79. https://doi.org/10.1007/s00027-014-0364-5

Carpenter, S. R., Cole, J. J., Pace, M. L., Batt, R., Brock, W. A., Cline, T., … Weidel, B. (2011). Early warnings of regime shifts: A whole-ecosystem experiment. *Science*, *332*(6033), 1079–1082. https://doi.org/10.1126/science.1203672

Chaffin, J. D., Kane, D. D., & Johnson, A. (2020). Effectiveness of a fixed-depth sensor deployed from a buoy to estimate water-column cyanobacterial biomass depends on wind speed. *Journal of Environmental Sciences*, *93*, 23–29. https://doi.org/10.1016/j.jes.2020.03.003

Christensen, J. P. A., Sand-Jensen, K., & Staehr, P. A. (2013). Fluctuating water levels control water chemistry and metabolism of a charophyte-dominated pond. *Freshwater Biology*, *58*(7), 1353–1365. https://doi.org/10.1111/fwb.12132

Codd, G. A., Morrison, L. F., & Metcalf, J. S. (2005). Cyanobacterial toxins: Risk management for health protection. *Toxicology and Applied Pharmacology*, *203*(3), 264–272. https://doi.org/10.1016/j.taap.2004.02.016

Corbel, S., Mougin, C., & Bouaïcha, N. (2014). Cyanobacterial toxins: Modes of actions, fate in aquatic and soil ecosystems, phytotoxicity and bioaccumulation in agricultural crops. *Chemosphere*, *96*, 1–15. https://doi.org/10.1016/j.chemosphere.2013.07.056

Cotterill, V., Hamilton, D. P., Puddick, J., Suren, A., & Wood, S. A. (2019). Phycocyanin sensors as an early warning system for cyanobacteria blooms concentrations: A case study in the Rotorua lakes. *New Zealand Journal of Marine and Freshwater Research*, *53*(4), 555–570. https://doi.org/10.1080/00288330.2019.1617322

Davis, T. W., Berry, D. L., Boyer, G. L., & Gobler, C. J. (2009). The effects of temperature and nutrients on the growth and dynamics of toxic and non-toxic strains of Microcystis during cyanobacteria blooms. *Harmful Algae*, *8*(5), 715–725. https://doi.org/10.1016/j.hal.2009.02.004

DelSontro, T., Beaulieu, J. J., & Downing, J. A. (2018). Greenhouse gas emissions from lakes and impoundments: Upscaling in the face of global change. *Limnology and Oceanography Letters*, *3*(3), 64–75. https://doi.org/10.1002/lol2.10073

Dodds, W. K., Bouska, W. W., Eitzmann, J. L., Pilger, T. J., Pitts, K. L., Riley, A. J., … & Thornbrugh, D. J. (2009). Eutrophication of US freshwaters: Analysis of potential economic damages. *Environmental Science & Technology*, *43*(1), 12–19. https://doi.org/10.1021/es801217q

Downing, J. A. (2010). Emerging global role of small lakes and ponds: Little things mean a lot. *Limnetica*, *29*(1), 9–24.

George, D. G., & Heaney, S. I. (1978). Factors influencing spatial-distribution of phytoplankton in a small productive lake. *Journal of Ecology*, *66*(1), 133–155. https://doi.org/10.2307/2259185

Gilbert, P. M. (2017). Eutrophication, harmful algae and biodiversity—Challenging paradigms in a world of complex nutrient changes. *Marine Pollution Bulletin*, *124*(2), 591–606. https://doi.org/10.1016/j.marpolbul.2017.04.027

Green, J. C. (2006). Effect of macrophyte spatial variability on channel resistance. *Advances in Water Resources*, *29*(3), 426–438. https://doi.org/10.1016/j.advwatres.2005.05.010

Hansen, A. M., Andersen, F. O., & Jensen, H. S. (1997). Seasonal pattern in nutrient limitation and grazing control of the phytoplankton community in a non-stratified lake. *Freshwater Biology*, *37*(3), 523–534. https://doi.org/10.1046/j.1365-2427.1997.00182.x

Karlsson-Elfgren, I., & Brunberg, A. K. (2004). The importance of shallow sediments in the recruitment of Anabaena and Aphanizomenon (Cyanophyceae). *Journal of Phycology*, *40*(5), 831–836. https://doi.org/10.1111/j.1529-8817.2004.04070.x

Kassambara, A. (2020). rstatix: Pipe-Friendly Framework for Basic Statistical Tests. R package version 0.6.0. Retrieved from https://cran.r-project.org/package=rstatix

Kelly, P. T., Renwick, W. H., Knoll, L., & Vanni, M. J. (2019). Stream nitrogen and phosphorus loads are differentially affected by storm events and the difference may be exacerbated by conservation tillage. *Environmental Science & Technology*, *53*(10), 5613–5621. https://doi.org/10.1021/acs.est.8b05152

Laas, A., Noges, P., Koiv, T., & Noges, T. (2012). High-frequency metabolism study in a large and shallow temperate lake reveals seasonal switching between net autotrophy and net heterotrophy. *Hydrobiologia*, *694*(1), 57–74. https://doi.org/10.1007/s10750-012-1131-z

Landsberg, J. H. (2002). The effects of harmful algal blooms on aquatic organisms. *Reviews in Fisheries Science*, *10*(2), 113–390. https://doi.org/10.1080/20026491051695

Lekki, J., Deutsch, E., Sayers, M., Bosse, K., Anderson, R., Tokars, R., & Sawtell, R. (2019). Determining remote sensing spatial resolution requirements for the monitoring of harmful algal blooms in the Great Lakes. *Journal of Great Lakes Research*, *45*(3), 434–443. https://doi.org/10.1016/j.jglr.2019.03.014

Loken, L. C., Crawford, J. T., Dornblaser, M. M., Striegl, R. G., Houser, J. N., Turner, P. A., & Stanley, E. H. (2018). Limited nitrate retention capacity in the Upper Mississippi River. *Environmental Research Letters*, *13*(7), 074030. https://doi.org/10.1088/1748-9326/aacd51

Loken, L. C., Crawford, J. T., Schramm, P. J., Stadler, P., Desai, A. R., & Stanley, E. H. (2019). Large spatial and temporal variability of carbon dioxide and methane in a eutrophic lake. *Journal of Geophysical Research-Biogeosciences*, *124*(7), 2248–2266. https://doi.org/10.1029/2019jg005186

McClain, M. E., Boyer, E. W., Dent, C. L., Gergel, S. E., Grimm, N. B., Groffman, P. M., … Pinay, G. (2003). Biogeochemical hot spots and hot moments at the interface of terrestrial and aquatic ecosystems. *Ecosystems*, *6*(4), 301–312. https://doi.org/10.1007/s10021-003-0161-9

Medeiros, A. S., Biastoch, R. G., Luszczek, C. E., Wang, X. A., Muir, D. C. G., & Quinlan, R. (2012). Patterns in the limnology of lakes and ponds across multiple local and regional environmental gradients in the eastern Canadian Arctic. *Inland Waters*, *2*(2), 59–76. https://doi.org/10.5268/iw-2.2.427

Møller, T. R., Rørdam, C. P., Moller, T. R., & Rordam, C. P. (1985). Species numbers of vascular plants in relation to area, isolation and age of ponds in Denmark. *Oikos*, *45*(1), 8–16. https://doi.org/10.2307/3565216

Moran, P. A. P. (1950). Notes on continuous stochastic phenomena. *Biometrika*, *37*(1–2), 17–23. https://doi.org/10.2307/2332142

Moreno-Ostos, E., Cruz-Pizarro, L., Basanta, A., & George, D. G. (2009). Spatial heterogeneity of cyanobacteria and diatoms in a thermally stratified canyon-shaped reservoir. *International Review of Hydrobiology*, *94*(3), 245–257. https://doi.org/10.1002/iroh.200811123

Ortiz, D., Palmer, J., & Wilkinson, G. (2019). Hypereutrophic lake sensor data during summer algae blooms in Iowa, USA, 2014–2018 ver 1. Environmental Data Initiative.

Ortiz, D., Palmer, J., & Wilkinson, G. (2020). Detecting changes in statistical indicators of resilience prior to algal blooms in shallow eutrophic lakes. *Ecosphere*, *11*(10), e03200. https://doi.org/10.1002/ecs2.3200

Ortiz, D., & Wilkinson, G. (2019). Hypereutrophic lake spatial sensor data during summer bloom, Swan Lake, Iowa, USA 2018 ver 1. Environmental Data Initiative.

Pebesma, E. J. (2004). Multivariable geostatistics in S: The gstat package. *Computers & Geosciences*, *30*(7), 683–691. https://doi.org/10.1016/j.cageo.2004.03.012

Pebesma, E. J. (2018). Simple features for R: Standardized support for spatial vector data. *The R Journal*, 10(1), 439–446. https://doi.org/10.32614/RJ-2018-009

Pellerin, B. A., Stauffer, B. A., Young, D. A., Sullivan, D. J., Bricker, S. B., Walbridge, M. R., … Shaw, D. M. (2016). Emerging tools for continuous nutrient monitoring networks: Sensors advancing science and water resources protection. *Journal of the American Water Resources Association*, 52(4), 993–1008. https://doi.org/10.1111/1752-1688.12386

R Core Team. (2020). *R: A language and environment for statistical computing*. R Foundation for Statistical Computing. Retrieved from https://www.R-project.org/

Read, J. S., Hamilton, D. P., Jones, I. D., Muraoka, K., Winslow, L. A., Kroiss, R., … Gaiser, E. (2011). Derivation of lake mixing and stratification indices from high-resolution lake buoy data. *Environmental Modelling & Software*, 26(11), 1325–1336. https://doi.org/10.1016/j.envsoft.2011.05.006

Rennella, A. M., & Quiros, R. (2006). The effects of hydrology on plankton biomass in shallow lakes of the Pampa Plain. *Hydrobiologia*, 556, 181–191. https://doi.org/10.1007/s10750-005-0318-y

Romo, S., Soria, J., Fernandez, F., Ouahid, Y., & Baron-Sola, A. (2013). Water residence time and the dynamics of toxic cyanobacteria. *Freshwater Biology*, 58(3), 513–522. https://doi.org/10.1111/j.1365-2427.2012.02734.x

Rychtecky, P., & Znachor, P. (2011). Spatial heterogeneity and seasonal succession of phytoplankton along the longitudinal gradient in a eutrophic reservoir. *Hydrobiologia*, 663(1), 175–186. https://doi.org/10.1007/s10750-010-0571-6

Schilder, J., Bastviken, D., van Hardenbroek, M., Kankaala, P., Rinta, P., Stotter, T., & Heiri, O. (2013). Spatial heterogeneity and lake morphology affect diffusive greenhouse gas emission estimates of lakes. *Geophysical Research Letters*, 40(21), 5752–5756. https://doi.org/10.1002/2013gl057669

Schoen, J. H., Stretch, D. D., & Tirok, K. (2014). Wind-driven circulation patterns in a shallow estuarine lake: St Lucia, South Africa. *Estuarine Coastal and Shelf Science*, 146, 49–59. https://doi.org/10.1016/j.ecss.2014.05.007

Serizawa, H., Amemiya, T., & Itoh, K. (2008). Patchiness in a minimal nutrient—Phytoplankton model. *Journal of Biosciences*, 33(3), 391–403. https://doi.org/10.1007/s12038-008-0059-y

Smith, C. D. (2018). *Temporal and spatial monitoring of cyanobacterial blooms at willow creek reservoir, North-Central Oregon*. Retrieved from U.S. Geological Survey Scientific Investigations Report

Solomon, C. T., Bruesewitz, D. A., Richardson, D. C., Rose, K. C., Van de Bogert, M. C., Hanson, P. C., … Zhu, G. (2013). Ecosystem respiration: Drivers of daily variability and background respiration in lakes around the globe. *Limnology and Oceanography*, 58(3), 849–866. https://doi.org/10.4319/lo.2013.58.3.0849

Song, K., & Burgin, A. J. (2017). Perpetual phosphorus cycling: Eutrophication amplifies biological control on internal phosphorus loading in agricultural reservoirs. *Ecosystems*, 20(8), 1483–1493. https://doi.org/10.1007/s10021-017-0126-z

Staehr, P. A., Christensen, J. P. A., Batt, R. D., & Read, J. S. (2012). Ecosystem metabolism in a stratified lake. *Limnology and Oceanography*, 57(5), 1317–1330. https://doi.org/10.4319/lo.2012.57.5.1317

Stanley, E. H., Collins, S. M., Lottig, N. R., Oliver, S. K., Webster, K. E., Cheruvelil, K. S., & Soranno, P. A. (2019). Biases in lake water quality sampling and implications for macroscale research. *Limnology and Oceanography*, 64(4), 1572–1585. https://doi.org/10.1002/lno.11136

Stockwell, J. D., Doubek, J. P., Adrian, R., Anneville, O., Carey, C. C., Carvalho, L., … Wilson, H. L. (2020). Storm impacts on phytoplankton community dynamics in lakes. *Global Change Biology*, 26(5), 2756–2784. https://doi.org/10.1111/gcb.15033

United States Environmental Protection Agency. (1993a). *Determination of Nitrate-Nitrite by Automated Colorimetry. Method 353.2 Revision 2.0*.

United States Environmental Protection Agency. (1993b). *Determination of Phosphorus by Semi-Automated Colorimetry. Method 365.1 Revision 2.0*.

United States Environmental Protection Agency. (1993c). *Determination of Total Kjeldahl Nitrogen by Semi-Automated Colorimetry Method 351.2, Revision 2.0*.

Van de Bogert, M. C., Bade, D. L., Carpenter, S. R., Cole, J. J., Pace, M. L., Hanson, P. C., & Langman, O. C. (2012). Spatial heterogeneity strongly affects estimates of ecosystem metabolism in two north temperate lakes. *Limnology and Oceanography*, 57(6), 1689–1700. https://doi.org/10.4319/lo.2012.57.6.1689

Verpoorter, C., Kutser, T., Seekell, D. A., & Tranvik, L. J. (2014). A global inventory of lakes based on high-resolution satellite imagery. *Geophysical Research Letters*, 41(18), 6396–6402. https://doi.org/10.1002/2014gl060641

Vilas, M. P., Marti, C. L., Adams, M. P., Oldham, C. E., & Hipsey, M. R. (2017). Invasive macrophytes control the spatial and temporal patterns of temperature and dissolved oxygen in a shallow lake: A proposed feedback mechanism of macrophyte loss. *Frontiers in Plant Science*, 8, 2097. https://doi.org/10.3389/fpls.2017.02097

Wilkinson, G. M., Carpenter, S. R., Cole, J. J., Pace, M. L., Batt, R. D., Buelo, C. D., & Kurtzweil, J. T. (2018). Early warning signals precede cyanobacterial blooms in multiple whole-lake experiments. *Ecological Monographs*, 88(2), 188–203. https://doi.org/10.1002/ecm.1286

Wu, X., Kong, F., Chen, Y., Qian, X., Zhang, L., Yu, Y., … Xing, P. (2010). Horizontal distribution and transport processes of bloom-forming Microcystis in a large shallow lake (Taihu, China). *Limnologica*, 40(1), 8–15. https://doi.org/10.1016/j.limno.2009.02.001

Wynne, T. T., & Stumpf, R. P. (2015). Spatial and temporal patterns in the seasonal distribution of toxic cyanobacteria in western Lake Erie from 2002–2014. *Toxins*, 7(5), 1649–1663. https://doi.org/10.3390/toxins7051649

Zhou, Y. T., Obenour, D. R., Scavia, D., Johengen, T. H., & Michalak, A. M. (2013). Spatial and temporal trends in lake Erie hypoxia, 1987–2007. *Environmental Science & Technology*, 47(2), 899–905. https://doi.org/10.1021/es303401b

SUPPORTING INFORMATION

Additional supporting information may be found online in the Supporting Information section.